THE JOURNAL OF BIOLOGICAL CHEMISTRY
Vol. 273, No. 52, Issue of December 25, pp. 35176–35184, 1998

Printed in U.S.A.

The Type I Keratin 19 Possesses Distinct and Context-dependent Assembly Properties*

(Received for publication, December 19, 1997, and in revised form, October 19, 1998)

Julie Fradette‡§, Lucie Germain‡¶, Partha Seshaiah‖, and Pierre A. Coulombe‖**

From the ‡Laboratoire de Recherche des Grands Brûlés/LOEX, Hôpital du Saint-Sacrement, Québec G1S 4L8, the Department of Surgery, Université Laval, Sainte-Foy, Québec, Canada, and the ‖Departments of Biological Chemistry and Dermatology, The Johns Hopkins University School of Medicine, Baltimore, Maryland 21205

Keratins (K), the cytoplasmic intermediate filament (IF) proteins of epithelial cells, are encoded by a multigene family and expressed in a tissue- and differentiation-specific manner. In human skin, keratinocytes of the basal layer of epidermis and the outer root sheath of hair follicles express K5 and K14 as their main keratins. A small subpopulation of basal cells exhibiting stem-cell like characteristics express, in addition, K19. At 40 kDa, this keratin is the smallest IF protein due to an exceptionally short carboxyl-terminal domain. We examined the assembly properties of K19 and contrasted them to K14 *in vitro* and *in vivo*. Relative to K5–K14, we find that K5–K19 form less stable tetramers that polymerize into shorter and narrower IFs *in vitro*. When transiently coexpressed in cultured baby hamster kidney cells, the K5 and K19 combination fails to form a filamentous array, whereas the K5–K14 and K8–K19 ones readily do so. Transient expression of K19 in the epithelial cell lines T51B-Ni and A431 results in its integration into the endogenous keratin network with minimal if any perturbation. Collectively, these results indicate that K19 possesses assembly properties that are distinct from those of K14 and suggest that it may impart unique properties to the basal cells expressing it in skin epithelia.

Keratins (K)[1] are intermediate filament (IF) proteins encoded by a large multigene family and expressed in epithelial tissues. The >30 known keratins (40–70 kDa) expressed in soft epithelia have been subdivided into type I (acidic, K9–K20) and type II (basic, K1–K8) based on DNA sequence homology and gene structure (1). Keratin filament assembly is a multistep process that begins with the formation of a type I–type II heterodimer (2), distinguishing them from most other IF proteins, which form homodimers. As a result, an epithelial cell must coordinately express at least one type I and type II keratin genes in order to assemble an IF network in its cytoplasm. Many keratin genes are in fact regulated in a pairwise, differentiation-specific manner, creating patterns that have been well conserved among mammalian species (1, 3). In stratified epithelia, for instance, the type II gene K5 and the type I genes K14 and K15 are expressed in the basal layer, whereas distinct combinations of type I and type II keratin genes are expressed in the differentiating suprabasal layers. A major function of keratin IFs in stratified epithelia is to contribute to the physical strength that is necessary to maintain their integrity in response to normal load of mechanical stress. This is particularly obvious in the epidermis and oral mucosa, as mutations affecting specific keratin proteins underlie several inherited blistering disorders such as epidermolysis bullosa simplex, epidermolytic hyperkeratosis, oral white sponge nevus, and others (2, 4, 5).

One of the most intriguing keratin is K19. At 40 kDa, this type I keratin is the smallest known IF protein (6, 7). The primary structure of human, bovine, and mouse K19 is highly conserved and made unique by virtue of an exceptionally short (13-residue long) tail domain at the carboxyl terminus (8–11). Otherwise, the length of the central rod domain (312 residues), a major determinant of IF polymerization (1, 2), is highly conserved, whereas the size of the non-helical, amino-terminal head domain (72 residues) is within the range observed for type I keratins (8–10). The primary structure of K19 is better related to the type I epidermal keratins than to K18, which predominates in simple epithelia (10). Still, the K19 gene is expressed in a variety of unrelated cell types in both simple and complex epithelia, such that there is no obvious relationship between the presence of K19 protein and the structure or function of an epithelial cell (10, 12–15). Although this combination of an unusual primary structure and heterogeneous distribution renders K19 particularly interesting, the function that it may perform remains unclear.

In adult human skin epithelia, K19 is found in a relatively small subset of keratinocytes in the basal layer and in Merkel cells, a minor population (<1%) of mechanosensory cells (Refs. 16 and 17 and references therein). These two cell types are functionally distinct and can be discriminated based on the specific reactivity of Merkel cells with antibodies directed against K18 and K20 (16, 18, 19). In human trunk skin, the K19-containing keratinocytes were found to localize to a distinct region of hair follicles known as the bulge, where they are confined to the basal layer of the outer root sheath. In the thicker glabrous epidermis of palms and soles, K19-containing keratinocytes are restricted to the deep portion of the rete ridges and are again confined to the basal layer (20). Such a distribution is intriguing, as both the bulge area of hair follicles and the deep portion of the epidermis in glabrous skin were

* This work was supported by National Science Foundation Grant MCB-9319560 and National Institutes of Health Grant AR44232 (to P. A. C.) and by Medical Research Council of Canada Grant MT-12087 (to L. G.). The costs of publication of this article were defrayed in part by the payment of page charges. This article must therefore be hereby marked "*advertisement*" in accordance with 18 U.S.C. Section 1734 solely to indicate this fact.

§ Recipient of a Studentship from the Medical Research Council of Canada.

¶ Recipient of a Scolarship from the Fonds de la Recherche en Santé du Québec. To whom reprint requests should be addressed: Laboratoire d'Organogénèse Expérimentale, Hôpital du Saint-Sacrement, 1050, Chemin Sainte-Foy, Québec, Canada, G1S 4L8. Tel.: 418-682-7696; Fax: 418-682-8000; E-mail: lucie.germain@chg.ulaval.ca.

** Recipient of a Junior Faculty Research Award from the American Cancer Society.

[1] The abbreviations used are: K, keratin; IF, intermediate filament; Gdn-HCl, guanidine HCl; PAGE, polyacrylamide gel electrophoresis; β-ME, β-mercaptoethanol; PCR, polymerase chain reaction; BHK, baby hamster kidney; CMV, cytomegalovirus; BS3, bis-(sulfosuccinimidyl) suberate.

shown to contain the reservoir of stem cells in adult skin (21, 22). Michel *et al.* (20) reported that many of the [^{3}H]thymidine label-retaining cells in these areas of mouse skin actually express K19, raising the possibility that a sizable fraction of the K19-expressing skin keratinocytes may be stem cells. Here we examine the assembly properties of K19 at the subunit, 10-nm filament, and cytoplasmic organization levels. The results of our studies suggest that K19 possesses distinct assembly properties that are likely to impact on the organization of keratin filaments in the progenitor cells of the skin.

EXPERIMENTAL PROCEDURES

Immunological Analyses—Frozen sections of human skin samples, cultured newborn foreskin keratinocytes (23), or cultured cell lines were analyzed by indirect immunofluorescence as described (20). The following primary antibodies were used: mouse monoclonal antibodies against K19 (Ks19.1, American Research Products, Belmont, MA, and clone A53-B/A2 from Sigma); K14 (Sigma and LL001; a gift from I. Leigh, Imperial Cancer Research Fund, London, UK); K18 (Ks18.174, American Research Products); K7 (LP5K, a gift from I. Leigh, Imperial Cancer Research Fund, London, UK); vimentin (V9, Sigma or anti-RLV, a gift from N. Marceau, Centre Hospitalier Universitaire de Québec, Quebec); K8 and K18 (L2A1; Ref. 24) and CAM5.2 coupled to fluorescein (Becton Dickinson, San Jose, CA); guinea pig and rabbit polyclonal antibodies against K5 (25); rabbit polyclonal antiserum anti-peptide directed against K14 (Ref. 26; a gift from N. Marceau, Quebec, Canada), against all K6 isoforms (27), and against K18 (28); and a guinea pig polyclonal antibody reacting against K8 and K18 (03-GP11, American Research Products). The goat secondary antibodies used were as follows: fluorescein-conjugated anti-guinea pig (Jackson ImmunoResearch, West Grove, PA), anti-mouse (Cedarlane, Hornby, Ontario, Canada), anti-rabbit (Chemicon, Temecula, CA), and rhodamine-conjugated anti-mouse (Chemicon). Negative controls consisted of omission of the primary antibody during the labeling reaction. For immunoelectron microscopy of methanol-fixed transfected BHK cells, a 10-nm gold goat anti-mouse antibody (British Biocell International, Cedarlane, Hornby, Ontario, Canada) was used for detection, and samples were fixed with 2.5% glutaraldehyde for 15 min, washed, post-fixed with 2% OsO_4 for 30 min, embedded in Epon and observed with a JEOL 1200 EX operated at 80 kV. Western blots were revealed by alkaline phosphatase-conjugated secondary antibodies (Sigma).

Cloning of Human K19 cDNA—The entire coding sequence for human K19 was obtained by reverse transcriptase-PCR using oligonucleotide primers designed from the published sequences (9, 10) and total RNA isolated from MCF-7 cells as described (29). The PCR product obtained was subcloned in plasmid pET-3d (30) for expression in bacteria. Several clones were subjected to dideoxy sequencing. The cDNA clone selected (see "Results") was transferred into GW1-CMV (31) for expression in cultured mammalian cells.

Keratin Expression and Purification—We used an *Escherichia coli* expression system based on the phage T7 RNA polymerase gene (30) to produce recombinant human keratins from plasmids pET-K19 (this study), pET-K5, and pET-K14 (32). Recombinant keratins were purified to near-homogeneity as described (31–33).

Heterotypic Complex Formation and Analysis—Purified recombinant type I and type II keratins were mixed in a ~45:55 molar ratio at ≈250 $\mu g \cdot ml^{-1}$, incubated for 1 h at room temperature, and fractionated by anion-exchange chromatography on a Pharmacia Mono Q column (31–33). Fractions containing type I-type II heterotypic complexes were pooled, dialyzed, and subjected to chemical cross-linking using BS3 (bis-(sulfosuccinimidyl) suberate; Pierce) as described (31, 33). Under these conditions, individual keratins do not cross-link into larger size products. Cross-linked products were resolved on a 4–16% gradient SDS-PAGE and stained with Coomassie Blue. Densitometry was performed using the public domain NIH Image 1.59 software[2] to estimate the relative yield of each major product of the reaction. For the competition assays, ≈300–435 μg of K14, K19, and K5 were mixed in a molar ratio of ≈1:1:1 to generate a final mixture having a 280 $\mu g \cdot ml^{-1}$ protein concentration. The mixture was analyzed by chromatography and SDS-PAGE as described above. Calculations and densitometric analyses were performed using NIH Image.

In Vitro Keratin Filament Assembly, Negative Staining, and Electron Microscopy—Mono Q fractions containing heterotypic keratin complexes were used for *in vitro* polymerization assays (32). Polymerization was achieved by dialysis of samples at 300 $\mu g \cdot ml^{-1}$ against 9 M urea, 50 mM Tris-HCl, 5 mM β-ME, pH 7.6, at room temperature and then against 3 mM Tris-HCl, 10 mM β-ME, pH 7.2, at 4 °C, for 16–24 h. In some experiments, the ionic strength of the final buffer was 50 mM Tris-HCl. Polymerized keratins were visualized by negative staining (1% uranyl acetate) on a Zeiss EM10A electron microscope (31). For filament length determination, negatives (magnification, × 20,000) were scanned and analyzed using the NIH image software. Measurements were made on a random sample of 74–117 filaments from two independent experiments. For filament width determination, 50 filaments were randomly selected from photographic prints (magnification, × 61,250) collated from three independent experiments. Statistical analyses were done using Student's t test. Polymerization efficiency was determined via a pelleting assay on the final assemblies as described (31, 33).

Transient Expression of Keratin cDNAs in Cultured Cells in Vitro—Keratin cDNAs were inserted into the GW1-CMV expression plasmid (31). pMK8 and pMK18 (kindly provided by B. Omary) are derivatives of the CMV promoter-based pMRB101 expression plasmid (34). For transient transfection assays, all cell lines were cultivated in media supplemented with 10% fetal bovine serum and antibiotics unless otherwise indicated. BHK-21 cells and NIH3T3 mouse fibroblasts were grown in Dulbecco's modified Eagle's medium, PtK2 (35), and A431 cells in Dulbecco's modified Eagle's medium:Ham's F12 (3:1) medium and T51B cells, an established cell line derived from adult rat liver as well as T51B-Ni, a subclone selected by prolonged exposure of the parental cell line to nickel subsulfide (Ref. 36; a gift from N. Marceau, Quebec, Canada) were cultivated in α- minimum Eagle's medium supplemented with 5% fetal bovine serum (Immunocorp.). Transfections were done on subconfluent cells grown on 22-mm^2 glass coverslips using the calcium phosphate precipitation method (31) or a polycation-mediated gene transfer using polyethylenenimine (Aldrich, Milwaukee, WI) (37). At 24–72 h post-transfection, cells were fixed with absolute methanol for 20 min at −20 °C and processed for indirect double immunofluorescence as described above. As routine controls, CMV-GW1 or mock-transfected cells were processed in parallel with the relevant antibodies. For the epithelial cell lines that already express endogenous keratins, we co-transfected vectors containing keratins cDNAs with limiting amount (1:9 ratio GFP:total DNA) of pEGFP-N1 vector (CLONTECH, Palo Alto, CA) and relied on the intrinsic fluorescence of the green fluorescence protein to identify transfected cells after fixation with 1% formaldehyde for 10 min and cold methanol for 20 min.

Quantitation of Epidermal Keratins in Transfected Cells—For quantitation of transfected keratins, BHK, PtK2, and A431 cells were seeded on 100-mm plates that contained one 22-mm^2 glass coverslip. BHK cells were cotransfected with the following CMV plasmid combinations: K5 and K14, K5 and K19, K14 and K19, or CMV vector alone. PtK2 and A431 cells were transfected with each of control CMV, CMV-K14 cDNA, and CMV-K19 cDNA plasmids. The amounts of DNA and the volume of precipitates were scaled up on a per surface area basis to maintain conditions similar to those prevailing in 35-mm culture dishes. At 26–30 h post-transfection, the glass coverslips were processed for staining to determine transfection efficiency. The remaining cells were recovered by scraping directly in gel loading buffer (total protein extracts). For SDS-PAGE/immunoblot analyses, known amounts of purified recombinant K14 or K19 (10, 20, 40, and 60 ng) were co-electrophoresed along with extracts prepared from transfected cells and blotted onto nitrocellulose. Blots were double-stained for the endogenous K8–18 (PtK2 cells) or vimentin (BHK cells) to ensure that equal amount of proteins were loaded in each lane. At each step, blots were scanned and densitometric analyses done using NIH image.

RESULTS

K19 Is Co-expressed with K5 and K14 in a Subset of Keratinocytes in Situ and in Vitro—Double immunofluorescence microscopy was performed to identify the type II keratins that occur in the subset of K19-positive basal keratinocytes. Our studies focused on the type II keratins K5, K6, K7 and K8, as these are known to occur in glabrous and hairy skin (3, 12, 38, 39). We did not attempt to localize either K1 and K2e, as these are restricted to the suprabasal differentiating layers in epidermis and in the uppermost segment of the hair follicle outer root sheath (see Refs. 40 and 41 and references therein). As expected (data not shown), we found that K19 co-localizes with

[2] Available on-line at the following address: http://rsb.info.nih.gov/nih-image.

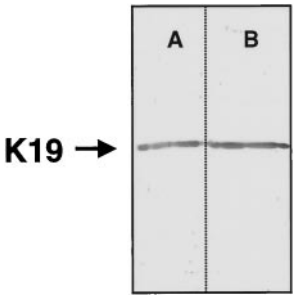

FIG. 1. **Immunological analysis of purified human recombinant K19.** Western blot analysis using a monoclonal antibody reacting against human K19. *A,* human recombinant K19 (50 ng). *B,* MCF-7 cell extract (~1.5 μg of total proteins). The purified recombinant protein co-migrates with endogenous (native) K19 from total extracts of MCF-7 cells.

K5 and K14 in the outermost (basal) cells of the bulge region of hair follicles (10, 42) and in the basal layer of newborn foreskin epidermis. We did not find evidence of co-expression of K19 with either K6 or K7 (data not shown), whereas a very scarce signal for K8 was detected in the hair bulge area, consistent with the relative paucity of Merkel cells in this region (16). In primary cultures of human foreskin keratinocytes, we find that K19 is expressed in a subset of cells (20) and co-localizes with K5, K6, and K14 (not shown). Under our culture conditions, only a proportion of K19-containing cells also express K8, and we do not detect immunoreactivity for K7 (data not shown). From these studies, we conclude that K5 is likely to be the major type II keratin partner for pairing and co-assembly with K19 in the relevant subset of human skin keratinocytes and that the type I K14 is also present in this cell population.

Characterization of the Human K19 cDNA Clone and Its Protein Product—We applied reverse transcriptase-PCR on total RNA from human MCF-7 breast adenocarcinoma cells to clone the coding sequence of K19. We identified a subclone whose nucleotide sequence is in complete agreement with that previously published by Eckert (9) with one exception. The PCR-mediated creation of a *Nco*I restriction site (CCATGG) at the start codon resulted in a Thr (ACT) → Ala (GCC) substitution at the first amino acid. When induced, BL21 (DE3) *E. coli* transformed with plasmid pET-K19 (see "Materials and Methods") express a ≈40-kDa protein that is retrieved in the inclusion body fraction and which co-purifies with acidic keratins on a Mono Q anion exchange column (31–33). Purified K19 reacts with a monoclonal antibody to K19 by Western blotting, and the positive recombinant antigen co-migrates with native K19 extracted from cultured human MCF-7 cells (Fig. 1). These data establish the validity of our cDNA clone as well as of the recombinant protein derived from it.

Comparing K5–K19 and K5–K14 Heterotypic Complex Formation in Vitro—To compare the formation of heterotypic complexes involving K5–K19 and K5–K14, these purified keratins were mixed in a predetermined ratio and subjected to established chromatography and chemical cross-linking assays (32, 33). When subjected to Mono Q chromatography at pH 8.1 in the presence of 6.5 M urea, purified type II epidermal keratins exist as monomers and elute at ~70–80 mM Gdn-HCl, designated as "peak 1," whereas purified type I epidermal keratins (also monomeric) elute at a higher salt concentration (~100–130 mM Gdn-HCl), designated as "peak 2." The sequential elution of type II and type I keratins under basic buffer conditions is consistent with their known surface charge (12). Mixtures of type I and type II keratins show a different elution profile as follows: heterotetramers elute at a yet higher salt concentration (~150–175 mM Gdn-HCl), designated as "peak 3", whereas heterodimers co-elute with type I monomers in peak 2 fractions (Ref. 33 and references therein).

When tested individually in the Mono Q chromatography assay, K19 elutes at the position characteristic for monomeric type I keratins (peak 2; data not shown). As expected, no dimer or tetramer is seen when purified K19 is subjected to cross-linking (data not shown). When mixed with K5 prior to chromatography, on the other hand, K19 shows an elution profile consistent with its recruitment in heterotypic complexes. Indeed, the majority of the K5 and K19 proteins elute as a 1:1 complex at a higher Gdn-HCl than either keratin alone, indicating efficient heterotypic complex formation (Fig. 2*A*). Consistent with the slightly less acidic character of K19 monomer compared with K14 (data not shown), the bulk of K5–K19 heterotypic complexes elute at ≈145–150 mM Gdn-HCl, whereas the peak of K5–K14 complex occurs at ≈155–160 mM Gdn-HCl (Fig. 2*A*). In addition, we find that relative to K5–K14, a small fraction of the K5 and K19 proteins co-elute significantly earlier in the Gdn-HCl gradient, in the so-called peak 2 fractions (Fig. 2*A*). This suggests that K5–K19 may not form heterotetramers with the same efficiency as K5–K14.

Chemical cross-linking using BS3 establishes that the major K5–K19 species formed under 6 M urea buffer conditions is a ≈240-kDa product, with a lesser amount of a ≈130-kDa product (Fig. 2*B*). As previously shown (*e.g.* Ref. 33), these species correspond to covalently cross-linked heterotetramers (46%) and heterodimers (38%) of keratins, respectively. Comparatively, the K5–K14 pair forms the ≈240-kDa heterotetramers with higher efficiency (70%). Furthermore, tetramers comprised of K5–K19 are destabilized to a greater extent when the urea concentration is raised to 8 M under otherwise identical conditions. Indeed, the yields of tetramer cross-links for K5–K19 and K5–K14 are lowered to 5 and 48%, respectively (Fig. 2*B*). Since the rod domains of human K19 and K14 feature comparable numbers of Lys residues (13 *versus* 18, respectively), it is unlikely that the difference seen in their behavior is due to a bias arising from the mechanism of cross-linking. This interpretation is further supported by the elution profile of K5–K19 and K5–K14 from the Mono Q column (Fig. 2*A*). Taken together, these data suggest that K19 can readily form heterotetramers in combination with K5 but that these are slightly less stable than those formed by K5–K14.

We next examined tetramer formation under conditions where K19 and K14 would have to compete for a limiting amount of K5. Purified K19, K14, and K5 were mixed in a ~1:1:1 ratio in the presence of 6.5 M urea, incubated for 1 h, and subjected to Mono Q chromatography. Consistent with the high efficiency with which K19 and K14 each pair with K5, the latter is almost entirely recruited (94%) to peak 3 fractions ("tetramer") (Fig. 3). The K5-containing heterotypic complexes elute as a single peak, suggesting the formation of mixed heterotetramers. Densitometry analysis of all the fractions making up peak 3 revealed the presence of a greater amount of K14 on a molar basis, such that it is enriched 1.7-fold compared with K19. As expected, this ratio is inverted in favor of K19 in the peak 2 fractions, which contain the molar excess of type I keratins (Fig. 3). These data suggest that K5 has a greater affinity for K14 compared with K19, a finding that may have implications for the regulation of K14 and K19 in skin epithelia *in vivo*.

Comparing K5–K19 and K5–K14 Filament Assembly Properties in Vitro—To assess filament formation *in vitro*, purified type I-type II heterotypic complexes were subjected to dialysis against standard epidermal assembly buffer and examined by negative staining and electron microscopy. The K5–K19 pair readily assembles into intermediate-sized filaments (Fig. 4), although less efficiently (75%) than the K5–K14 pair (>90%) as

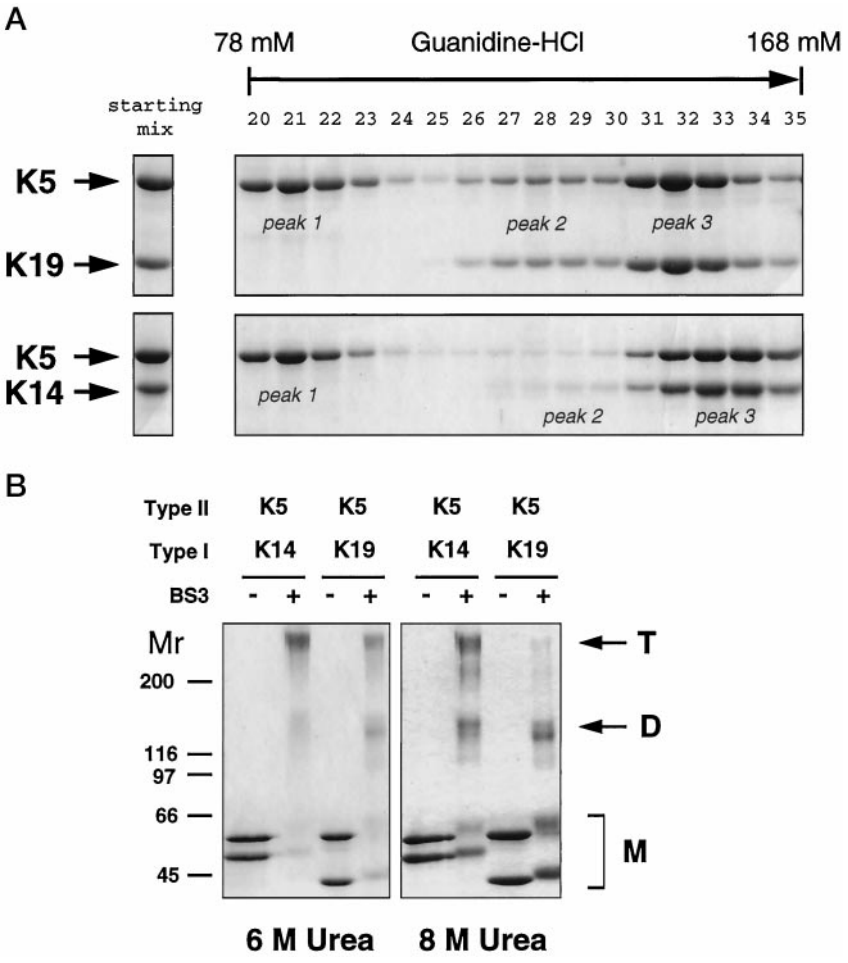

FIG. 2. *A,* elution profiles of recombinant keratins during anion-exchange chromatography. Purified K5 and K19 (*top*) and K5 and K14 (*bottom*) were mixed in a 55:45 ratio (see "Materials and Methods"), applied to a Mono Q anion-exchange chromatography column, and eluted over a 0–200 mM linear gradient of Gdn-HCl. Aliquots were analyzed by SDS-PAGE followed by staining with Coomassie Blue. *Peak 1*, excess type II keratins; *peak 2*, type I keratins and/or heterodimers of type I–II keratins; *peak 3*, heterotetramers of type I–II keratins. As shown previously (32), K5–K14 forms heterotypic complexes with high efficiency and which elutes as a single peak (*peak 3*). The K5–K19 mixture also readily forms heterotypic complexes, of which a small fraction elutes at a lower Gdn-HCl concentration (*peak 2*). *B,* chemical cross-linking of type I-type II keratin heterotypic complexes. Type I-type II heterotypic complexes isolated by anion-exchange chromatography were dialyzed against 25 mM sodium phosphate buffer containing either 6 or 8 M urea at pH 7.4. The cross-linking agent BS3 was added to keratin complexes (200 $\mu g \cdot ml^{-1}$) at a final concentration of 5 mM and the reaction stopped after 1 h. Cross-linked products (4 μg of proteins) were resolved on a 4–16% gradient SDS-PAGE and stained with Coomassie Blue. *T,* heterotetramers (~240 kDa); *D,* heterodimers (~135 kDa); and *M,* monomers. Although the K5–K19 combination forms tetramers with high efficiency under 6 M urea buffer conditions, these are more readily destabilized than the K5–K14 ones when the concentration of urea is raised to 8 M.

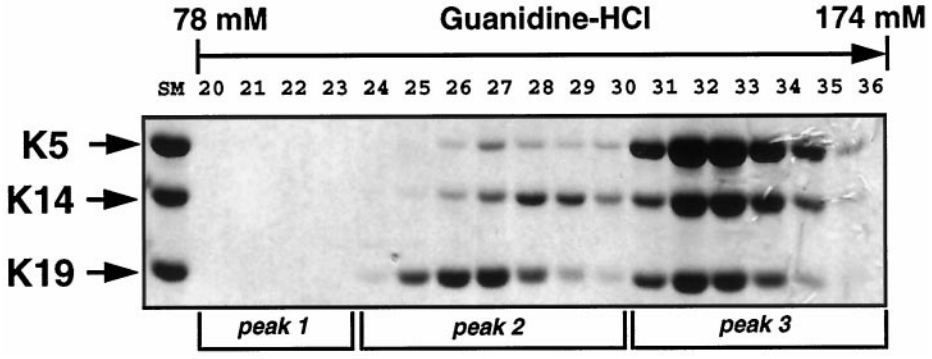

FIG. 3. **Assessing K19 tetramer-forming properties in a competitive environment *in vitro*.** For the competition assay, ≈300–435 μg of purified recombinant K14, K19, and K5 were mixed in a molar ratio of ≈1:1:1 to generate a final mixture having a 280 $\mu g \cdot ml^{-1}$ protein concentration. After incubation at room temperature for 1 h, the mixture was subjected to anion-exchange chromatography and eluted over a 0–200 mM linear gradient of Gdn-HCl. Fractions were analyzed by SDS-PAGE and Coomassie Blue staining. *Peak 1* represents the elution position of type II keratins; *peak 2*, the excess of type I keratins; and *peak 3*, the heterotypic complexes containing the three keratins. Determination of the protein ratio in the starting mix (*SM*) and in *peak 3* fractions shows that compared with K14, K19 has a 1.7-fold lower affinity for K5.

shown by a pelleting assay (data not shown). The K5–K19 filaments are significantly narrower than the K5–K14 ones (8.4 ± 0.1 nm *versus* 9.9 ± 0.1 nm, respectively; mean ± S.E.). Although it is consistent with the mass difference between K19 (40 kDa) and K14 (50 kDa), this smaller diameter could also reflect a smaller number of subunits per cross-section, a possibility that we did not investigate further. The average length of K5–K19 filaments (1.1 ± 0.1 μm) is shorter than that of K5–K14 filaments (2.0 ± 0.1 μm), a statistically significant difference ($p < 0.01$). It is likely that the sampling for these measurements is biased toward short filaments. Still, the numbers obtained reflect a trend that is readily detectable from a qualitative inspection of K5–K14 and K5–K19 assemblies (Fig. 4).

As predicted from our theoretical understanding of the polymerization of fibrous polymers (43), shorter filaments may arise following mechanisms as distinct as increased nucleation, decreased rate of elongation, or decreased stability of the polymer at steady state (44). We did not address these various possibilities at an experimental level. However, the lower efficiency of K5–K19 assembly compared with K5–K14 (as measured under assembly conditions optimal for epidermal keratins (45, 46) implies the existence of a higher concentration of unpolymerized proteins at steady state and supports the idea that K5–K19 filaments are less stable than K5–K14 ones. We ex-

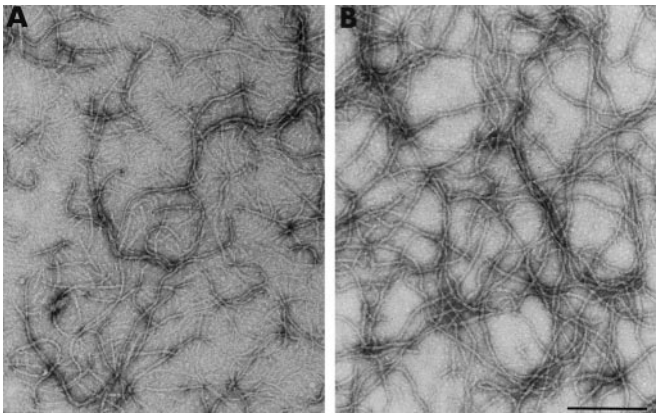

FIG. 4. **Electron microscopy of *in vitro* reconstituted keratin filaments.** Purified heterotypic complexes of K5 and K19 (*A*) and K5 and K14 (*B*) were subjected to dialysis against keratin assembly buffer (see "Materials and Methods") for several hours. The K5–K19 filaments obtained were slightly shorter and narrower than the K5–K14 ones. *Bar,* 200 nm.

amined assembly under increased ionic strength buffer conditions (50 mM Tris-HCl), which are optimal for the *in vitro* polymerization of wild-type K8–K18 (47) and truncated forms of K5–K14 proteins (48). Under such conditions, K5–K14 typically form ball-like aggregates of filaments, whereas K5–K19 form a mixture of looser aggregates and bundles in which multiple filaments are intertwined around one another (data not shown). We conclude from these studies that K5–K19 can readily polymerize under standard epidermal keratin assembly buffer conditions *in vitro* but that the resulting filaments are shorter than K5–K14 ones, perhaps as a result of a lesser stability.

Assembly Properties of K19 in Non-epithelial Cells in Culture—We compared the assembly properties of various keratin combinations involving K5 and K8 as type II keratins and K19, K14, and K18 as type I keratins in transfected BHK-21 cells. This cell line has a type III (vimentin and desmin) but lacks a keratin IF network (49), enabling us to examine the ability of combinations of type I–type II keratin to polymerize *de novo* in the cytoplasm of a living cell. Upon co-transfection, the majority of cells (>90%) co-expressing K5 and K19 do not show a filamentous array but a combination of dots distributed throughout the cytoplasm and aggregates preferentially located around the nuclei (Fig. 5, *A* and *A′*). In contrast and as previously reported (31), a majority of transfected cells (~70%) co-expressing K5 and K14 show bundles of keratin filaments extending throughout the cytoplasm (Fig. 5, *B, B′,* and *C*). We examined BHK cells at times ranging from 24 to 48 h after transfection and did not observe significant differences in the proportion of cells showing aggregated *versus* filamentous organization. We could not detect any obvious difference in the organization of the vimentin network in K5–K19- and K5–K14-transfected cells (data not shown). Expression of the K5–K19 and K5–K14 plasmid combinations in NIH 3T3 cells produce a very similar outcome (data not shown).

We compared the K19 and the K14 protein levels in BHK cells transfected with the K5–K19 or K5–K14 plasmid combinations (see "Materials and Methods") and found that they were comparable (Fig. 6*A*). Moreover, transfection of various molar ratios of K5:K19 plasmids (up to 5:1) did not improve filament forming potential in BHK cells. These data suggest that it is unlikely that the K5–K19 aggregates are produced as the result of K19 overexpression. Electron microscopy of double-transfected BHK cells shows that the large aggregates that are immunopositive for K19 are made of non-filamentous proteins (Fig. 6*B*). Collectively these data indicate that under our

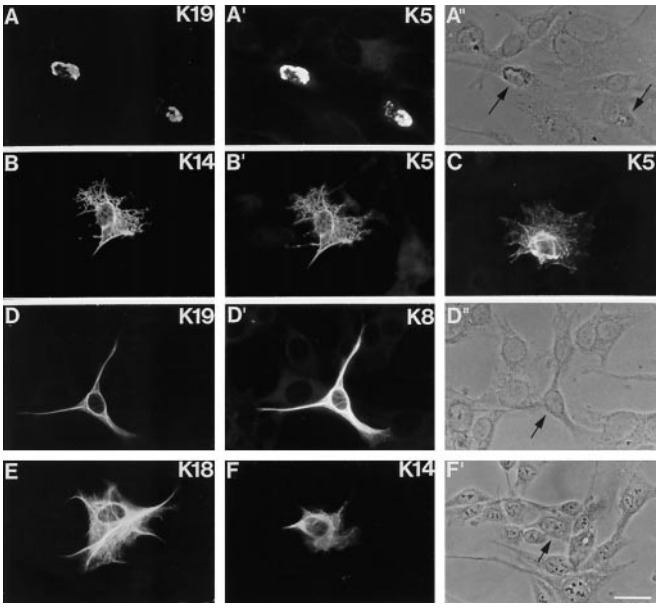

FIG. 5. **Co-expression of type I and type II keratin cDNAs in cultured BHK-21 cells.** Cells were fixed and double-immunofluorescence labelings were performed at 24–48 h after transfection. The antigens detected are indicated in the *upper right corner* of each micrograph. *Frames A, A′,* and *A″,* co-expression of the K5–K19 pair led to the production of aggregates containing both keratins. *A″* is a phase contrast micrograph showing the morphology of the transfected cells shown in *A* (see *arrows*). *Frames B, B′,* and *C,* co-expression of the K5–K14 pair gave rise to the formation of a filament network, as shown in these two examples. *Frames D, D′,* and *D″,* co-expression of K8–K19 produced filaments with a marked tendency to form bundles (again, the phase contrast image of the transfected cell is shown in *D″* (see *arrow*)). *Frame E,* co-expression of K8 and K18 led to formation of a well extended array of thin filaments throughout the cytoplasm. *Frames F* and *F′,* co-expression of K8–K14 led to a less well defined filamentous array. *Bar, A, C, D,* and *F,* 27 μm; *B* and *E,* 37 μm.

transfection conditions, and in contrast to the K5–K14, K5–K16, and K6–K14 plasmid combinations (this study and Ref. 31), co-expression of K5 and K19 does not give rise to a filamentous array in cultured BHK-21 cells.

We next examined whether K8, the major type II keratin gene co-expressed with K19 in simple epithelia, is a "better" pairing partner for the latter in transfected BHK cells. We found that in contrast to K5–K19, only ~12% of cells co-transfected with K8–K19 show aggregates (not shown). Among the other cells, ~33% show a dispersed filamentous array in a fashion analogous to K5–K14, whereas ~55% show thick bundles of filaments (Fig. 5, *D* and *D′*). By comparison, we found that ~60% of BHK cells co-transfected with K8 and K18 plasmids show a well extended network of filaments (Fig. 5*E*), whereas ~20% show large bundles of filaments (data not shown). Finally, 30% of the BHK cells transfected with K8 and K14 plasmids featured a filament network (Fig. 5*F*). These results establish that as is the case *in vitro* (47, 50–52), the K19 cDNA clone gives rise to a polymerization-competent keratin when paired with K8 in an *in vivo* like setting.

Transient Expression of K19 in Selected Epithelial Cell Lines Leads to Its Integration into the Pre-existing Keratin Network—Since the K5–K19 pair seemed unable to form filaments *de novo* in fibroblastic cells, we tested the ability of K19 to integrate into the pre-existing keratin network of an epithelial cell. We transfected the K19 cDNA into the T51B and T51B-Ni epithelial cell lines derived from rat liver and which express K8, K14, and vimentin but are negative for K19. In addition, T51B-Ni cells express K18 and features a more extended keratin network (36). In either cell line, transient expression of the K19 cDNA leads to integration of K19 protein into the endog-

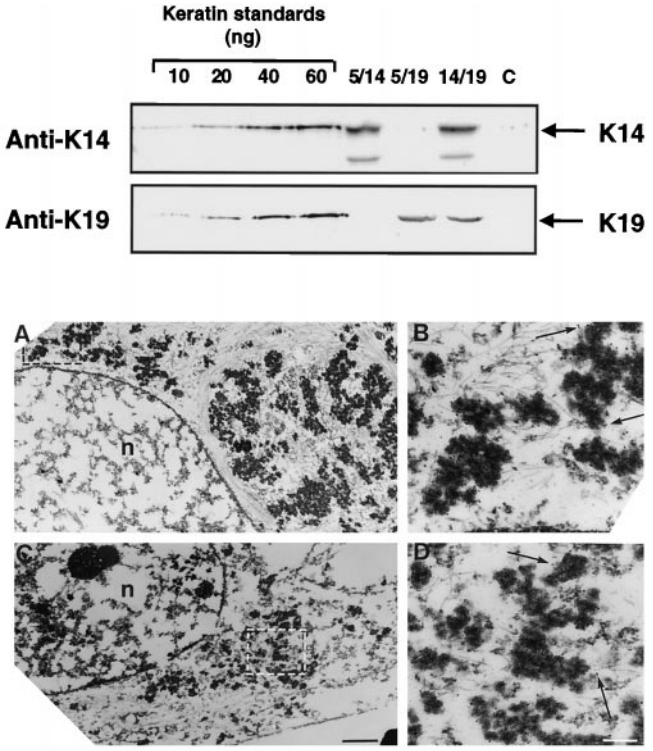

FIG. 6. *Top,* quantification of human keratin levels in transfected BHK cells. Western blot analysis using anti-K14 (*top*) and anti-K19 (*bottom*) antibodies to detect transfected keratin proteins. At 30 h after transfection, BHK cells were scraped in loading buffer and total proteins resolved by SDS-PAGE along with known amounts (10, 20, 40,and 60 ng) of recombinant purified K19 or K14. Densitometric analysis indicates that similar levels of K14 and K19 were expressed following transfection in BHK cells. *Bottom,* electron microscopy of K19-transfected BHK cells. Transfection of K5 and K19 cDNAs (*A* and *B*) or of K19 cDNA alone (*C* and *D*) into cultured BHK cells. *Frames B* and *D* are high magnification micrographs of the regions boxed in *frames A* and *C*, respectively. Immunogold labeling (10 nm, *arrows*) with an anti-K19 antibody reveals the unpolymerized nature of these K19-containing aggregates. *Bars:A* and *C,* 1 μm; *B* and *D,* 200 nm.

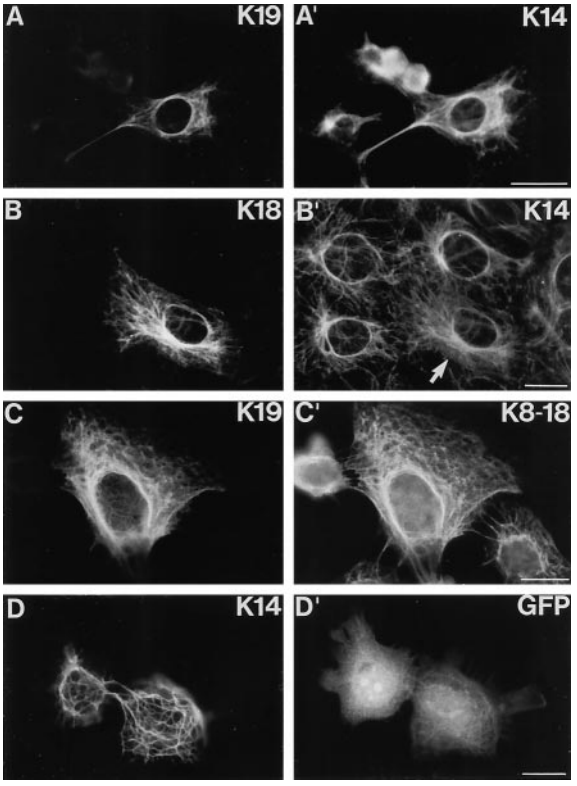

FIG. 7. **Transient expression of type I keratin cDNAs in T51B-Ni and A431 epithelial cell lines.** Cells were fixed and double-immunofluorescence labelings were performed at 24–48 h after transfection. The antigens detected are indicated in the *upper right corner* of each micrograph. *Frames A* and *A′,* T51B-Ni cells transfected with K19 and double-stained for endogenous K14. *Frames B* and *B′,* T51B-Ni cells transfected with K18 and double-stained for endogenous K14. *Frames C* and *C″,* A431 cells transfected with K19 and double-stained for endogenous K8–K18. *Frames D* and *D″,* A431 cells doubly-transfected with the K14 and a green fluorescent protein (*GFP*) reporter cDNA to unequivocally identify cells expressing the transfected cDNAs (see "Materials and Methods"). In all instances the transfected proteins integrated within the existing keratin IF network. *Bars,* 15 μm.

enous network in >70% of the transfected cells (Fig. 7, *A* and *A′*; T51B-Ni). Similarly, transfection of the K18 cDNA results in a K18 protein-containing filamentous array in >80% of transfected cells (Fig. 7, *B* and *B*'; T51B-Ni).

We next examined the behavior of transfected K19 in the A431 human epidermoid carcinoma cell line, which expresses K5, K6, K7, and K8 as their main type II keratins (12). Under our culture conditions, A431 cells express K18 at high levels, are negative for K19, and show sporadic expression of K14 (only ~10% of cells). Transient expression of the K19 (Fig. 7, *C and C′*) and K14 (Fig. 7, *D* and *D′*) cDNAs results in a filamentous pattern for 80 and 95% of transfected A431 cells, respectively, without disruption of the endogenous K8–18 network. Quantitation of transfected keratins by Western blot analysis demonstrates that K19 protein is expressed to the same level as the transfected K14 in this cell line (not shown). These studies establish that as expected of a wild-type keratin, newly synthesized K19 can incorporate into a well extended keratin IF array in these epithelial cell lines without perturbing it in an obvious fashion.

Transient Expression of K19 Causes a Collapse of the Keratin Network in PtK2 Epithelial Cells—We transfected K19 cDNA into the well characterized kidney rat kangaroo PtK2 cell line, whose well extended K8–K18 filament network makes it attractive for the examination of keratin assembly properties (*e.g.* Refs. 31 and 53–55). PtK2 cells transfected with CMV-K19 display a very striking phenotype. In more than 80% of transfected cells, indeed, expression of K19 results in the appearance of aggregates (Fig. 8, *A* and *B*) that stain positively with antibodies directed against endogenous K8–K18 (Fig. 8, *A′* and *B′*). In contrast, and as shown previously (31), human K14 protein integrates into the pre-existing K8–K18 network without disrupting it in 94% of transfected PtK2 cells (Fig. 8, *C* and *C′*).

The observations made in PtK2 cells are surprising since K8 is a "natural" partner for K19 *in vivo,* and these two keratins form an IF array when co-transfected in BHK cells (Fig. 5). Again, we compared the levels of exogenous keratins in transfected PtK2 cells and found that on average, K19 is expressed 5-fold more than K14 (not shown). It may be, therefore, that the unexpected phenotype seen in K19-expressing PtK2 cells is due to its expression at significantly higher levels. In support of this possibility, co-transfection of K8 and K19 produces a filamentous array in 70% of transfected PtK2 cells (Fig. 8*D*), and transfection of the K18 plasmid alone results in the production of clumps that correlate with a relatively abundant expression as judged from immunofluorescence staining (not shown). In contrast to K8, however, cotransfection of K5 and K19 fails to improve the filament-forming properties of the latter, since 75% of transfected PtK2 cells show either dots or clumps (Fig. 8*E*). Although our observations suggest that the PtK2 cell line can be sensitive to imbalances between type I and type II keratin protein levels, this phenomenon appears to be keratin-specific. The results obtained in this cell line support the notion

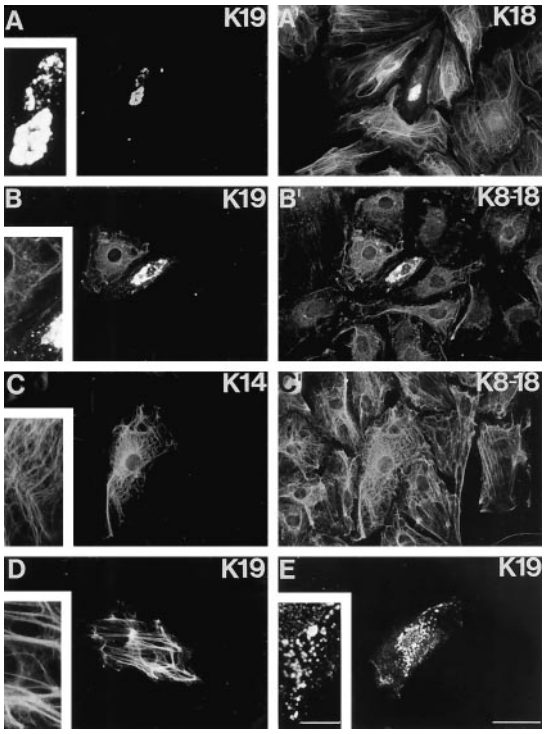

FIG. 8. **Transient expression of keratin cDNAs in cultured PtK2 cells.** Cultured epithelial PtK2 cells transiently transfected with human keratin cDNAs. At 24–72 h post-transfection, cells were fixed and processed for double-immunofluorescence labeling. The antigens detected are indicated in the *upper right corner* of each micrograph. *Frames A, A′, B,* and *B′,* cells transfected with the K19 cDNA and double-stained for endogenous K8–K18. *Frames C* and *C,* cells transfected with the K14 cDNA and double-stained for endogenous K8–K18. Note that in contrast to K14, expression of K19 results in aggregates disrupting the endogenous network. *Frames D* and *E,* cells cotransfected with the K8–K19 cDNAs (*frame D*) and K5–K19 cDNAs (*frame E*). Co-expression of K8, but not K5, "rescues" the disruption normally produced by K19 expression. *Insets* show magnification of a portion of the transfected cell. *Bars* are 50 μm; *insets* are 15 μm.

that K14 and K19 behave differently when co-expressed with K5.

DISCUSSION

There is increasing experimental evidence supporting the notion that although a general function of keratin IFs is to impart mechanical resilience to cells and tissues, various keratins possess different properties that are exploited in specific ways by the epithelial cells expressing them. For instance, the keratin pairs K5–K14, K1–K10, K6–K16, and K8–K18 have intrinsic properties that clearly distinguish them *in vitro* and that relate to their organization *in vivo* (31, 33, 46, 47, 55–59). In a significant step, direct support for this notion has recently been obtained through keratin replacement experiments performed in transgenic mice. Indeed, Hutton *et al.* (60) showed that human K18 is not able to fully rescue the severe phenotype associated with a null mutation in the K14 gene of mouse (61) under conditions where an exogenous epidermal keratin protein can. Similar studies in progress show that although it does so more efficiently than K18, human K16 cannot entirely rescue the mouse K14 null phenotype either.[3] Future efforts along these lines should firm up the evidence substantiating the existence of a significant relationship between keratin protein expression, filament network organization and regulation, and epithelial function.

Here we report that the human type I keratin 19, which is distinct by virtue of an extremely short tail domain (see Introduction), has properties that are distinct from those of K14 *in vitro* and *in vivo*. We believe that may potentially translate into a distinct keratin filament organization in the subset of skin keratinocytes that co-express K5, K14, and K19 *in vivo*. Relative to K5–K14 and under standard epidermal keratin assembly conditions *in vitro*, indeed, K5–K19 forms less stable tetramers that polymerize into shorter and narrower filaments with a 20% lower efficiency. Whereas numerous mechanisms could account for these differences, our *in vitro* findings suggest that a slightly lower stability of the K5–K19 polymer is potentially one of them (see "Results"). To our surprise, we also found that co-expression of K5 and K19 in two non-epithelial cell lines (BHK; NIH3T3) does not give rise to the formation of IFs as assessed by electron microscopy. This finding is at variance with the outcome of K5 and K19 co-polymerization *in vitro*, the co-expression of K8 and K19 in the same non-epithelial cell hosts (this study; see Refs. 50 and 51), and the expression of K19 in A431 cells, an epidermal cell line that features K5 and K8 as type II keratins. Of relevance, Hutton *et al.* (60) reported that expression of human K18 within the basal layer of transgenic mouse epidermis causes the formation of K5–K18 containing protein aggregates in the absence but not in the presence of endogenous K14. Again, this finding contrasts with the assembly behavior of purified recombinant human K5 and K18 *in vitro*, which produce long filaments and no aggregates (60). Collectively, our studies suggest that the impact of K19 expression upon the organization of keratin IFs is context-dependent, in that it likely depends upon the complement of keratin proteins, their abundance, or the complement of IF-associated and IF-regulating proteins present in the host cell.

Prior to our study, the assembly properties of K19 had for the most part been compared with those of K18, the major type I keratin with which it is co-expressed in simple epithelia. These studies showed that K19 is capable of forming typical IFs *in vitro* and *in vivo* when paired with K8, the major type II keratin present in those cells (47, 50–52). How the intrinsic properties of K19 compare with those of K18 remains unclear, however. In an elegant *in vitro* study, Hofmann and Franke (52) demonstrated that K18 and K19 are distinct in their affinity, polymerization kinetics, and properties of the filaments formed when paired with K8. In particular, they found that K8–K19 filaments display a significantly lower viscosity and appear shorter when examined by electron microscopy (see Fig. 7*A* in Ref. 52). In earlier studies, Lu and Lane (50) had found that when expressed via retroviral vectors in NIH3T3 cells, K8–K18 were able to form a more extended array of filaments compared with K8–K19. A different conclusion was reached by Bader *et al.* (51), however, whose experiments involved stably transfected fibroblasts, and more recently by Magin *et al.* (62) who, from their electron microscopy analysis of the uterine epithelium in K18 null mice, concluded that the morphological features of K8–K19 IFs were indistinguishable from K8–K18. The absence of consensus among all these studies, including ours, may simply reflect the notion that as speculated above, the assembly properties of individual keratins are modulated by the co-assembly partner(s) involved, the complement of keratin-associated and keratin-regulating proteins, or other features particular to each cell type. It is reasonable to conclude, then, that as is potentially the case in skin keratinocytes, the presence of K19 in simple epithelial cells may under some conditions promote a distinct organization of keratin IFs.

Recent work from Oshima and colleagues (63) and Omary and colleagues (64) showed that K18 and K19 are substrates for caspases, which are proteases involved in programmed cell death. Given that caspase-mediated cleavage occurs at the

[3] R. Paladini and P. A. Coulombe, unpublished data.

VEVD sequence motif located in the linker sequence between subdomains 2A and 2B, the resulting truncated K19 would likely behave as a dominant negative mutant (2). We did not see the nuclear changes characteristic of apoptosis in K5–K19 expressing fibroblasts, and the K5–K14 combination gave rise to filament arrays in a majority of transfected fibroblasts despite the occurrence of a highly related motif (VEMD) in linker L12 of K14 protein. Thus, we do not think that this mechanism accounts for our findings in transfected fibroblasts. On the other hand, we believe that the lack of an extended tail domain in K19 may likely contribute to specify the intrinsic assembly properties revealed in ours and other studies. This speculation is supported by experimental evidence implicating the tail domain of type I keratins such as K14 and K18 as playing a role in filament stability (47, 48, 50).

Our demonstration that K14 and K19 possess distinct properties leads to the speculation that the latter may promote a distinct organization of the keratin IF network in the relevant subset of basal skin keratinocytes. Michel *et al.* (20) recently extended the original findings of Stasiak *et al*. (10) in showing that a fraction of the K19-expressing basal cells in mouse skin are thymidine label-retaining cells, an operational criteria for stem cell character. This K19-positive subpopulation of cells localizes to the deep portion of rete ridges in the epidermis of glabrous human skin and the bulge portion of hair follicles in hairy skin (10, 20, 65). Interestingly, a subset of "K14-low," less differentiated basal cells in the outermost "basal" layer of the hair follicle outer root sheath has been described by one of us (66), and these cells have been postulated to serve as progenitors for both the hair follicle outer root sheath and the epidermis. Electron microscopy studies in progress in one of our laboratories (L. G.) confirmed the existence of these peculiar basal cells in the bulge region of human hair follicles (data not shown). Of note, there is no evidence for large keratin aggregates in keratinocytes localized in regions associated with K19 expression (66).[4] Taken together, these observations raise the possibility that in addition to their ability to retain thymidine label, the subset of K19-expressing basal keratinocytes may be less differentiated, express K14 at lower levels, and show a distinct organization of keratin IFs. Further studies will be required to address this intriguing possibility.

Expression of K19 occurs in a number of epithelial settings and frequently correlates with a phenomenon of "plasticity" in epithelial cell fate or function (10, 65). In contrast to many of the keratin genes expressed in the epidermis (2, 4, 5), mutations that affect the primary sequence and function of K19 have not yet been discovered in the human population. Moreover, introduction of a null mutation in the K19 gene of mouse has no obvious consequence for the morphogenesis and homeostasis of skin and other epithelia, at least under basal conditions.[5] The function of K19 thus remains to be defined. Further characterization of the morphology, properties, and function of the relevant subpopulation of skin epithelial cells in K19 null mice may provide clues for the function of K19 in this tissue.

Acknowledgments—We are very grateful to Drs. Normand Marceau for providing cell lines and antibodies; M. Bishr Omary for providing antibodies and cDNAs; Irene Leigh and Elaine Fuchs for providing antibodies; Claude Marin and Aristide Pusterla for photographic and electron microscopy assistance, respectively; and Dr. Olivier Bousquet for helpful discussions. We also thank Drs. Gabriel Gosselin, Jean-Guy Laberge, Jean-Marc Laliberté, and Alphonse Roy for providing skin specimens.

[4] J. Fradette and L. Germain, unpublished data.
[5] Drs. M. Taketo and Y. Tamai, personal communication.

REFERENCES

1. Fuchs, E., and Weber, K. (1994) *Annu. Rev. Biochem.* **63,** 345–382
2. Coulombe, P. A. (1993) *Curr. Opin. Cell Biol.* **5,** 17–29
3. O'Guin, W. M., Schermer, A., Lynch, M., and Sun, T. T. (1990) in *Cellular and Molecular Biology of Intermediate Filaments* (Goldman, R. D., and Steinert, P. M., eds) pp. 301–334, Plenum Publishing Corp., New York
4. McLean, W. H. I., and Lane, E. B. (1995) *Curr. Opin. Cell Biol.* **7,** 118–125
5. Fuchs, E. (1997) *Mol. Biol. Cell* **8,** 189–203
6. Wu, Y.-J., and Rheinwald, J. G. (1981) *Cell* **25,** 627–635
7. Moll, R., von Bassewitz, D. B., Schultz, U., and Franke, W. W. (1982) *Differentiation* **22,** 25–40
8. Bader, B. L., Magin, T. M., Matzfeld, M., and Franke, W. W. (1986) *EMBO J.* **5,** 1865–1875
9. Eckert, R. L. (1988) *Proc. Natl. Acad. Sci. U. S. A.* **85,** 1114–1118
10. Stasiak, P. C., Purkis, P. E., Leigh, I. M., and Lane, B. (1989) *J. Invest. Dermatol.* **92,** 707–716
11. Lussier, M., Ouellet, T., Lampron, C., Lapointe, L., and Royal, A. (1989) *Gene (Amst.)* **85,** 435–444
12. Moll, R., Franke, W. W., Schiller, D. L., Geiger, B., and Krepler, R. (1982) *Cell* **31,** 11–24
13. Bartek, J., Taylor-Papadimitriou, J., Miller, N., and Millis, R. (1985) *Int. J. Cancer* **36,** 299–306
14. Heid, H. W., Moll, I., and Franke, W. W. (1988) *Differentiation* **37,** 137–157
15. Su, L., Morgan, P. R., Thomas, J. A., and Lane, E. B. (1993) *J. Oral Pathol. & Med.* **22,** 183–189
16. Moll, I. (1994) *Cell Tissue Res.* **277,** 131–138
17. Lacour, J. P., Dubois, D., Pisani, A., and Ortonne, J. P. (1991) *Br. J. Dermatol.* **125,** 535–542
18. Moll, R., Moll, I., and Franke, W. W. (1984) *Differentiation* **28,** 136–154
19. Fradette, J., Godbout, M.-J., Michel, M., and Germain, L. (1995) *Biochem. Cell Biol.* **73,** 635–639
20. Michel, M., Török, N., Godbout, M.-J., Lussier, M., Gaudreau, P., Royal, A., and Germain, L. (1996) *J. Cell Sci.* **109,** 1017–1028
21. Lavker, R. M., and Sun, T.-T. (1982) *Science* **215,** 1239–1241
22. Cotsarelis, G., Sun, T. T., and Lavker, R. M. (1990) *Cell* **61,** 1329–1337
23. Germain, L., Rouabhia, M., Guignard, R., Carrier, L., Bouvard, V., and Auger, F. A. (1993) *Burns* **2,** 99–104
24. Chou, C.-F., Riopel, C. L., Rott, L. S., and Omary, M. B. (1993) *J. Cell Sci.* **105,** 433–444
25. Lersch, R., Stellmach, V., Stocks, C., Giudice, G., and Fuchs, E. (1989) *Mol. Cell. Biol.* **9,** 3685–3697
26. Royal, I., Grenier, A., Mailhot, D., and Marceau, N. (1995) *Exp. Cell Res.* **220,** 171–177
27. McGowan, K., and Coulome, P. A. (1998) *J. Cell Biol.* **143,** 469–486
28. McCormick, M. B., Kouklis, P., Syder, A., and Fuchs, E. (1993) *J. Cell Biol.* **122,** 395–407
29. Paladini, R. D., Takahashi, K., Gant, T. M., and Coulombe, P. A. (1995) *Biochem. Biophys. Res. Commun.* **215,** 517–523
30. Studier, F. W., Rosenberg, A. H., Dunn, J. J., and Dubendorff, J. W. (1990) *Methods Enzymol.* **185,** 60–89
31. Paladini, R. D., Takahashi, K., Bravo, N. S., and Coulombe, P. A. (1996) *J. Cell Biol.* **132,** 381–397
32. Coulombe, P., and Fuchs, E. (1990) *J. Cell Biol.* **111,** 153–169
33. Wawersik, M., Paladini, R. D., Noensie, E., and Coulombe, P. A. (1997) *J. Biol. Chem.* **272,** 32557–32565
34. Ku, N. O., and Omary, M. B. (1994) *J. Cell Biol.* **127,** 161–171
35. Franke, W. W., Schmid, E., Osborn, M., and Weber, K. (1978) *Eur. J. Cell Biol.* **17,** 392–411
36. Blouin, R., Swierenga, S. H. H., and Marceau, N. (1992) *Biochem. Cell Biol.* **70,** 1–9
37. Boussif, O., Lezoualc'h, F., Zanta, M. A., Mergny, M. D., Scherman, D., Demeneix, B., and Behr, J. P. (1995) *Proc. Natl. Acad. Sci. U. S. A.* **92,** 7297–7301
38. Takahashi, K., Paladini, R. D., and Coulombe, P. A. (1995) *J. Biol. Chem.* **270,** 18581–18592
39. Bader, B. L., and Franke, W. W. (1990) *Differentiation* **45,** 109–118
40. Rothnagel, J. A., Dominey, A. M., Dempsety, L. D., Longley, M. A., Greenhalgh, D. A., Gagne, T. A., Huber, M., Frenk, E., Hohl, D., and Roop, D. R. (1992) *Science* **257,** 1128–1130
41. Collin, C., Moll, R., Kubicka, S., Ouhayoun, J. P., and Franke, W. W. (1992) *Exp. Cell Res.* **202,** 132–141
42. Lane, E. B., Wilson, C. A., Hughes, B. R., and M., L. I. (1991) *Ann. N. Y. Acad. Sci.* **642,** 197–213
43. Oosawa, F., and Asakura, S. (1975) *Thermodynamics of the Polymerization of Proteins*, Academic Press, New York
44. Stewart, M. (1993) *Curr. Opin. Cell Biol.* **5,** 3–11
45. Steinert, P. M., and Idler, W. W. (1976) *J. Mol. Biol.* **108,** 547–567
46. Eichner, R., Sun, T.-T., and Aebi, U. (1986) *J. Cell Biol.* **102,** 1767–1777
47. Hatzfeld, M., and Weber, K. (1990) *J. Cell Sci.* **97,** 317–324
48. Wilson, A. K., Coulombe, P. A., and Fuchs, E. (1992) *J. Cell Biol.* **119,** 401–414
49. Quinlan, R. A., and Franke, W. W. (1982) *Proc. Natl. Acad. Sci. U. S. A.* **79,** 3452–3456
50. Lu, X., and Lane, E. B. (1990) *Cell* **62,** 681–696
51. Bader, B. L., Magin, T. M., Freudenmann, M., Stumpp, S., and Franke, W. W. (1991) *J. Cell Biol.* **115,** 1293–1307
52. Hofmann, I., and Franke, W. W. (1997) *Eur. J. Cell Biol.* **72,** 122–132
53. Albers, K., and Fuchs, E. (1987) *J. Cell Biol.* **105,** 791–806
54. Rorke, E. A., Crish, J., and Eckert, R. L. (1992) *J. Invest. Dermatol.* **98,** 17–23
55. Paramio, J. M., and Jorcano, J. L. (1994) *Exp. Cell Res.* **215,** 319–331
56. Blessing, M., Rüther, U., and Franke, W. W. (1993) *J. Cell Biol.* **120,** 743–755
57. Kartasova, T., Roop, D. R., Holbrook, K., and Yuspa, S. H. (1993) *J. Cell Biol.* **120,** 1251–1261
58. Paramio, J. M., Casanova, M. L., Alonso, A., and Jorcano, J. L. (1997) *J. Cell*

Sci. **110,** 1099–111
59. Paladini, R. D., and Coulombe, P. A. (1998) *J. Cell Biol.* **142,** 1035–1051
60. Hutton, E., Paladini, R. D., Yu, Q. C., Yen, M.-Y., Coulombe, P. A., and Fuchs, E. (1998) *J. Cell Biol.* **143,** 487–499
61. Lloyd, C., Yu, Q.-C., Cheng, J., Turksen, K., Degenstein, L., Hutton, E., and Fuchs, E. (1995) *J. Cell Biol.* **129,** 1329–1344
62. Magin, T. M., Schröder, R., Leitgeb, S., Wanninger, F., Zatloukal, K., Grund, C., and Melton, D. W. (1998) *J. Cell Biol.* **140,** 1441–1451
63. Caulin, C., Salvesen, G. S., and Oshima, R. G. (1997) *J. Cell Biol.* **138,** 1379–1394
64. Ku, N. O., Liao, J., and Omary, M. B. (1997) *J. Biol. Chem.* **272,** 33197–33203
65. Bartek, J., Bartkova, J., Schneider, J., Taylor-Papadimitriou, J., Kovarik, J., and Rejthar, A. (1986) *Eur. J. Clin. Oncol.* **22,** 1441–1452
66. Coulombe, P. A., Kopan, R., and Fuchs, E. (1989) *J. Cell Biol.* **109,** 2295–2312